Can Hail and Rain Nucleate Cloud Droplets?

Prasanth Prabhakaran,[1,2,†] Stephan Weiss,[1] Alexei Krekhov,[1] Alain Pumir,[3,1] and Eberhard Bodenschatz[1,2,4,*]
[1]Max Planck Institute for Dynamics and Self-Organization, 37077 Göttingen, Germany
[2]Institute for Nonlinear Dynamics, University of Göttingen, 37073 Göttingen, Germany
[3]Laboratoire de Physique, Ecole Normale Supérieure de Lyon,
Université de Lyon 1 and Centre National de la Recherche Scientifique, 69007 Lyon, France
[4]Laboratory of Atomic and Solid-State Physics and Sibley School of Mechanical and Aerospace Engineering,
Cornell University, Ithaca, New York 14853, USA
(Received 29 May 2017; published 22 September 2017)

We present results from moist convection in a mixture of pressurized sulfur hexafluoride (liquid and vapor), and helium (gas) to model the wet and dry components of the Earth's atmosphere. To allow for homogeneous nucleation, we operate the experiment close to critical conditions. We report on the nucleation of microdroplets in the wake of large cold liquid drops falling through the supersaturated atmosphere and show that the homogeneous nucleation is caused by isobaric cooling of the saturated sulfur hexafluoride vapor. Our results carry over to atmospheric clouds: falling hail and cold rain drops may enhance the heterogeneous nucleation of microdroplets in their wake under supersaturated atmospheric conditions. We also observed that under appropriate circumstances settling microdroplets form a rather stable horizontal cloud layer, which separates regions of super- and subcritical saturation.

DOI: 10.1103/PhysRevLett.119.128701

A key process in clouds is nucleation, i.e., the formation of condensation nuclei under supersaturated conditions that eventually grow to form micrometer size cloud droplets [1]. It is well known that the cloud dynamics and the formation of precipitation size droplets are strongly influenced by the concentration and the properties of the aerosol particles [1]. In fact, the complex interactions between flow turbulence, droplets and ice particles of various sizes, and phase transitions makes it difficult to model clouds [2–5]. Inspired by laboratory experiments [6,7], several field experiments were conducted to enhance precipitation in clouds. In two seminal studies [8,9] dry ice was dropped on top of developing cumulus clouds, which in most cases triggered explosive cloud growth with significant rainfall in its neighborhood. Since then several investigations have been carried out to understand the dynamics associated with nucleation in clouds with and without seeding [1,10–12].

In this Letter, we report experimental findings on nucleation in a multiphase convection system consisting of sulfur hexafluoride (SF_6) and helium (He). This system aims to mimic atmospheric conditions with SF_6 existing in both liquid and vapor phases, thus acting as the moist component. Helium is added to mimic the dry component in the Earth's atmosphere. The advantage of using SF_6 is that a relatively small supersaturation is required to trigger homogeneous nucleation [13].

The nucleation of SF_6 microdroplets in the wake of cold SF_6 drops falling from the top plate (Fig. 1) is our main finding. We argue that the induced isobaric cooling in the wake increases locally the saturation ratio, and therefore triggers homogeneous nucleation. We show that a similar mechanism carries over to atmospheric clouds, where falling ice particles (hail) and/or large, cold rain drops can enhance the heterogeneous nucleation rate of droplets. Furthermore, in the experiment, under appropriate conditions, we observe the nucleated SF_6 droplets forming a rather stable horizontal cloud layer, separating regions of sub- and supercritical saturation, just as in an atmospheric cloud layer.

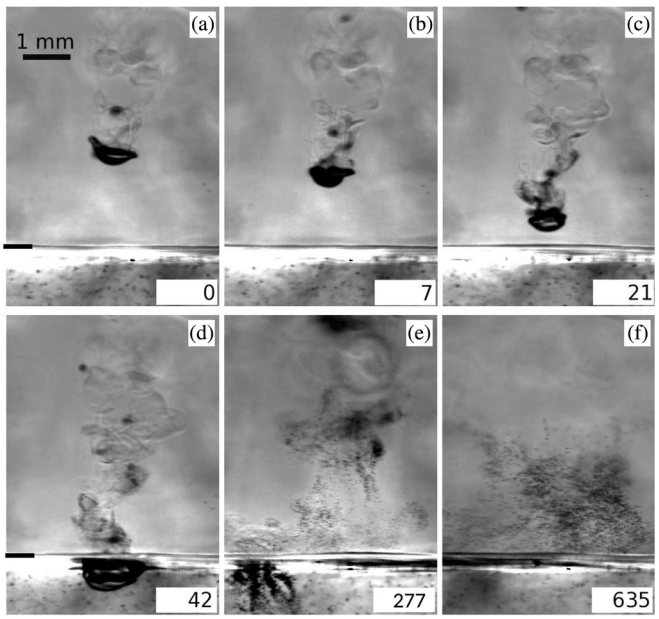

FIG. 1. Contrast enhanced image sequence of an SF_6 drop falling through the gaseous SF_6-He layer. The black mark on the left indicates the position of the liquid-vapor interface located at about 6 mm from the bottom plate. The time stamp (in ms) for each of these figures is indicated at the bottom right corner.

 © 2017 American Physical Society

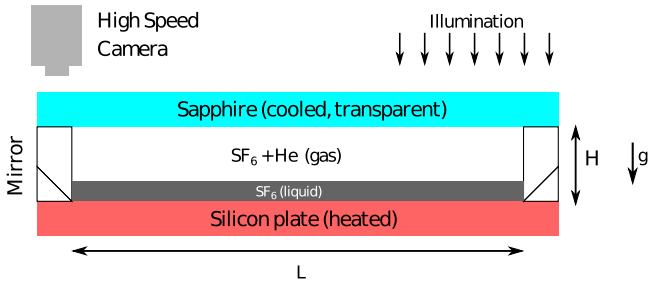

FIG. 2. Schematic of the experimental setup. Mirrors are embedded into the side wall on all four sides of the square cell. For clarity only two mirrors are shown.

The experiments were performed in a high-pressure convection apparatus that has previously been used to study pattern formation close to the onset of convection [14–16]. The main part of the apparatus is the convection cell (Fig. 2) that consists of two horizontal plates, $H = (22.6 \pm 0.5)$ mm apart from each other. The side walls of the cell were made of acrylic with a square cross section of side length $L = (61.65 \pm 0.01)$ mm. The top plate, a 9.5 mm thick monocrystalline sapphire providing optical access, was kept horizontal and was cooled by circulating water on its top surface. The bottom plate was a 9.5 mm thick monocrystalline silicon disc that was heated with an Ohmic film heater at its bottom side. The top and bottom plate temperatures were regulated to ± 10 mK of the set temperature. In order to provide visual access from the side, two sets of mirrors were embedded into the acrylic side walls at 45°. One set of mirrors provides optical access to the top half and the other set to the bottom half of the cell (Fig. 2). Image acquisition was done at 140 fps at a resolution of 2048×2048 [17].

The bottom plate was heated to a temperature T_b, while the top plate was maintained at $T_t < T_b$. The conditions were such that a layer of liquid SF_6 formed at the bottom of the cell. At the liquid-gas interface, SF_6 evaporated, rose, and condensed underneath the top plate creating a thin liquid film, which continuously underwent a Rayleigh-Taylor-like instability. As a consequence, drops of SF_6 dripped and fell through the gas layer into the liquid SF_6 pool at the bottom.

Figure 1 shows a deformed drop with a lateral diameter about 1 mm, accompanied by a smaller drop falling through the gaseous SF_6-He atmosphere. Since these drops originated from the liquid layer at the top plate, their temperature is close to T_t. Local inhomogeneities in the gas temperature, hence in the refractive index, are visible in the wake of the cold drop by shadowgraphy [Figs. 1(a)–(d)]. In the near wake of the deformed drop, the shed vortices mix the cold gas from the boundary layer with the warmer ambient gas as shown in Figs. 1(a)–(d), thus locally altering the saturation ratio and temperature. Particularly in Fig. 1(c), the enhanced contrast in the near wake is due to the nucleation of microdroplets which become visible in Fig. 1(d). Please note that the large drop enters the liquid pool without a visible splash. These microdroplets continue to grow in size by condensation of SF_6 vapor from their supersaturated neighborhood till they fall into the liquid pool [Figs. 1(e) and 1(f) and movie in [18]]. Note that for fixed experimental conditions the number of nucleated microdroplets vary strongly for different falling drops (see movie in [18]). This points to a nonuniform distribution of SF_6 vapor due to the turbulent convection in the gaseous layer [20,21].

In the experiment shown in Fig. 1, the temperatures at the top and bottom plates were $T_t = 40.00\,°\mathrm{C}$ and $T_b = 44.00\,°\mathrm{C}$, and the pressure was $p = (46.9 \pm 0.1)$ bar. Based on Dalton's law, we estimate the mole fraction of He inside the gaseous layer to be $x_{\mathrm{He}} \approx 26\%$. We found that the nucleation of microdroplets in the wake of a falling drop was observed when T_b was sufficiently close to the critical temperature of SF_6 (45.57°C) at fixed $T_b - T_t$. As we show below, this can be attributed to the lowering of the critical supersaturation required for nucleation as the critical temperature is approached.

Classical nucleation theory [22,23] provides an estimate for the rate of formation of liquid phase critical droplets ("embryos"), J, as a function of the saturation ratio, S. By convention [1], the detectable rate of nucleation is taken to be $J_c = 1\ \mathrm{cm}^{-3}\,\mathrm{s}^{-1}$. This leads to a definition of a critical saturation ratio S_c. The corresponding critical size r_c that needs to be exceeded for a sustained droplet growth is calculated using Kelvin's equation [18]. For the mean temperature $T_m = 42\,°\mathrm{C}$, using SF_6 parameters [24–26], we find $S_c = 1.000815$, $r_c = 21.2$ nm and the time to establish the steady-state nucleation rate $\tau = 1.3\ \mu$s (see [18]). Using Maxwell's model (diffusion limited growth), we estimate the time for growth by condensation from an initial radius of r_c to $r = 10\ \mu$m to 41.5 ms [18]. This time agrees remarkably well with the time difference between Figs. 1(a) and 1(d), i.e., the time interval between the cooling of the ambient gas at a certain location and the first appearance of microdroplets in its neighborhood.

In the experiment, the SF_6 vapor close to a falling cold drop is cooled from an initial temperature T to $T - \Delta T$ due to diffusive and convective heat transport from the drop's surface. As a consequence, the saturation ratio becomes $S = p_v(T)/p_s(T - \Delta T)$, where ΔT represents the temperature difference between the ambient gas and the wake. For $T_m = 42\,°\mathrm{C}$ of saturated SF_6 vapor, i.e., $p_v(T) = p_s(T)$, a $\Delta T = 0.04$ K is sufficient to reach $S = S_c$, in comparison to a $\Delta T = 0.57$ K at $T_m = 30\,°\mathrm{C}$. Note that the cooling in the wake to $\Delta T > 0.04$ K is attainable, given that the temperature of the cold falling drop was initially 2 K below the mean temperature in the cell. To show this, we estimate the cooling, i.e., the temperature difference Δ between the ambient gas and a drop of diameter d, falling at its terminal velocity U_t, in a gas layer of temperature $T_a(z)$ decreasing linearly with height. We find

$$\Delta = \Delta_0 e^{-At} + \frac{\beta U_t}{A}(1 - e^{-At}) \quad \text{with} \quad A = \frac{6\lambda \mathrm{Nu}}{\rho_l d^2 c_{p,l}} \qquad (1)$$

where $\Delta_0 = \Delta(t = 0)$, $\beta = dT_a/dz$, Nu is the Nusselt number (ratio between convective and conductive heat transfer), λ is the thermal conductivity of the ambient gas, and ρ_l, $c_{p,l}$ are the density and the specific heat of the liquid, respectively (see [18] for additional details).

In Fig. 1, the diameter of the cold SF_6 drops detaching from the top plate $d \approx 0.5$ mm. From the images, we found that the terminal velocity of the drop $U_t \approx 7$ cm/s was reached after about a 2 mm fall from the top. Drops reach the liquid layer above the bottom plate in about 0.2 s. Using the material parameters of SF_6 at $T_m = 42\,°\mathrm{C}$ [26] and an empirical relation between the drop Reynolds number and Nu [27], we find $\mathrm{Re} \approx 600$ and $\mathrm{Nu} \approx 26$, and thus from Eq. (1), $1/A \approx 0.18$ s. Let us assume that when the drop attains its terminal velocity ($t = 0$), it has the same temperature as its ambient, i.e., $\Delta_0 = 0$. To account for convective mixing in the gas layer, we choose $\beta = 0.5$ K/cm, which is four times smaller than the applied temperature gradient of 2 K/cm across the gas layer. Equation (1) predicts that $\Delta = 0.1$ K and 0.2 K at $t \approx 30$ ms and 60 ms, respectively, which is well before the drop enters the liquid pool.

The cooling ΔT in the wake of the drop is determined by the heat transfer rate from the ambient gas to the cold drop and as such is a function of Re of the falling drop and the streamwise distance from the drop's surface. Simulations at $\mathrm{Re} > 300$ [28] of the instantaneous temperature distribution in the near wake show that the separated shear layers retain up to 20% of Δ till about 2 droplet diameters downstream. The settling cold drop, with $\Delta = 0.2$ K, therefore induces isobaric cooling of the ambient wake by $\Delta T \approx 0.04$ K at $t = 60$ ms which is sufficient to trigger homogeneous nucleation at $T_m = 42\,°\mathrm{C}$. The cooling in the near wake is enhanced with further fall of the drop.

Please note that this is a simple estimate. In fact, the ΔT required to trigger homogeneous nucleation also depends on the distribution of SF_6 vapor in the boundary layer and the wake. Moreover, additional complexities arise due to the mixing of parcels of different temperature and vapor content. We here assume that the SF_6 vapor content is constant and saturated at T_m. As a consequence, the level of supersaturation estimated by isobaric cooling with constant SF_6 vapor content gives an upper bound.

If the bottom plate is covered by a liquid layer, the SF_6 vapor in the gas is on average saturated or slightly supersaturated due to the continuous supply of vapor from the liquid pool below. As a consequence, any sufficiently large microdroplet would continue to grow till it reaches the liquid layer. The saturation ratio S, of SF_6 vapor inside the cell can be lowered by eliminating the liquid layer above the bottom plate while keeping all the other parameters fixed, thus cutting off the vapor supply. In such cases, $S \geq S_c$ in the upper, colder part of the cell, while $S < S_c$ in the warmer lower part. Figure 3 displays the observations in the lower part of the cell in the absence of a liquid layer on the bottom plate. The microdroplets were nucleated in the wake of drops falling from the top plate, similar to that in Fig. 1, except that sustained nucleation in the wake was observed only above a certain height [see Figs. 3(a) and 3(b) and movie in [18]]. This height marks the horizontal interface where $S \approx S_c$. In the region above this interface, the nucleated microdroplets grow in size and below the interface they evaporate (see movie in [18]). Figure 3(b) shows a layer of microdroplets suspended in the gas layer. The dark band in Fig. 3(c) represents the time averaged cloud layer and it suggests that the layer has a well-defined base, similar to the clouds in the Earth's atmosphere. The mean

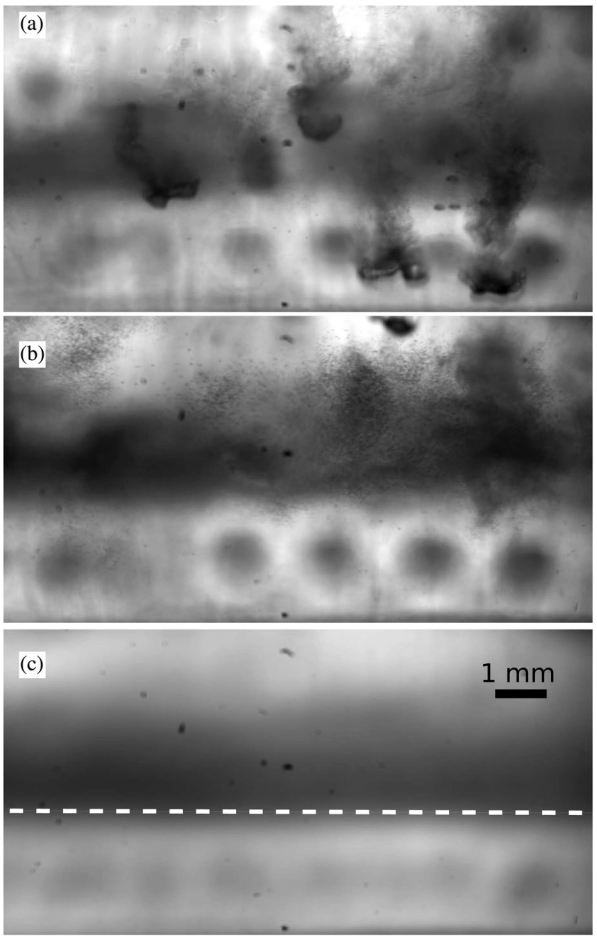

FIG. 3. Cloud layer: Formation of a cloud layer in the lower part of the cell in the absence of a liquid layer at the bottom plate. $T_b = 45.00\,°\mathrm{C}$, $T_t = 36.00\,°\mathrm{C}$, $p = 44.9$ bar. The dark circular patches in the lower part of the image are due to the drops attached to the top plate. (a) Drops from the top plate falling through the gas layer. (b) Microdroplets nucleated in the wake and suspended in the gas. Image taken 760 ms after (a). (c) Time averaged image over 1550 frames (≈11 s). The white dashed line represents the mean position of the base of the cloud layer and thus vertically separates areas of supercritical (above) and subcritical saturation (below).

position of this base is marked in Fig. 3(c). Below this interface no sustained nucleation was observed.

Let us now compare the conditions in the Earth's atmosphere with those in the experiment and check under which conditions the present observations can be carried over. For homogeneous nucleation of liquid water in the moist air for the temperature range $-30\,°\mathrm{C} \leq T_a \leq +30\,°\mathrm{C}$ the critical saturation ratio S_c varies between 7 and 3. However, the supersaturation that develops in natural clouds rarely exceeds a few percent [1]. Consequently, water droplets do not form by homogeneous nucleation but rather by heterogeneous nucleation on atmospheric aerosol particles [1]. The number of particles capable of growing, denoted as cloud condensation nuclei (CCN) grows with supersaturation, $s = S - 1$, typically with a power law dependence on s [1].

Consider moist cloudy air at temperature T and $S \approx 1$ that contains a certain amount of the CCN. When a large cold water drop (or hail particle), falls through a warmer ambient air, it will cause isobaric cooling of the air in its wake, similar to the drops in our experiment. This results in locally enhanced supersaturation that can create more CCN, and an increase in the number of microdroplets. For example, to attain a supersaturation $s = 2\%$ by isobaric cooling starting from the saturated vapor, a temperature drop of $0.21\ \mathrm{K} \leq \Delta T \leq 0.34\ \mathrm{K}$ (varies almost linearly) for the temperature range $-30\,°\mathrm{C} \leq T_a \leq +30\,°\mathrm{C}$ is needed.

In a cloud, the ambient temperature surrounding a falling rain drop increases as the drop approaches the cloud base. We assume that the temperature variation within a cloud is linear with a typical moist adiabatic lapse rate $\approx 0.005\ \mathrm{K/m}$ [29]. Then for a raindrop at its terminal velocity U_t, the steady state temperature difference between the ambient air and the drop, $\Delta = \Delta_\infty = \beta U_t / A$, is calculated using Eq. (1). For a drop of diameter 1 mm (4 mm), one finds Δ_∞ is about 0.07 K (0.95 K) (see [18]). The Δ_∞ for the 1 mm drop is too small to cause significant supersaturation in its wake. However, for a drop of diameter 4 mm, close to the largest values in the size distribution [1], the resulting cooling in the wake $\Delta T = 0.2\Delta_\infty = 0.19\ \mathrm{K}$ is sufficient to attain about 1.5% supersaturation and thus leads to enhanced nucleation in its wake.

Let us consider an ice particle falling through an environment with the ambient temperature above 0 °C. Because of the fusion enthalpy, the cooling ΔT in its wake is larger than for a rain drop of the same diameter. It is known that the temperature inside a particle composed of a mixture of liquid water and ice is nearly homogeneous due to the shear enhanced mixing inside the particle [30]. As a consequence the temperature of the ice particle would not increase until it is completely melted. The heat transfer rate is also known to depend on the shape of the ice particle [30]. Let us assume a spherical particle of uniform density. To account for liquid condensation on the surface, we further assume a 25% larger heat transfer rate between the particle and its surroundings than for the liquid drop [31]. Based on these considerations an ice particle of 1 mm diameter ($\mathrm{Re} \approx 230$) would travel ≈450 m and a particle of diameter 5 mm ($\mathrm{Re} \approx 3600$) would travel ≈2000 m before it is completely melted. The corresponding maximum Δ_∞ for these particles are about 2.2 K and 10 K, respectively (see [18] for details). As a consequence, the local supersaturation would be around 2%–10% in the near wake of the particle taking into account $\Delta T = 0.2\Delta_\infty$. This enhanced supersaturation would activate more nuclei and hence increase the concentration of microdroplets in the warmer part of the cloud. We infer that in comparison to a cold drop, significantly higher levels of supersaturation are attained in the wake of a hail. Note, that for an aerosol particle with radius $\leq 1\ \mu\mathrm{m}$, the time required to activate the CCN is smaller than the Kolmogorov time scale in the clouds [1].

The estimates here are based on idealized conditions. In a (convective) cloud, the dynamics is more complicated due to the presence of updrafts, variable lapse rates due to nonuniform latent heat release from condensation or glaciation, and inhomogeneous mixing due to entrainment of ambient dry air into the cloud [32]. Nevertheless, the results from our model system and the analysis presented in this Letter suggest that in clouds, the cooling induced by a falling hail particle can indeed lead to the nucleation of droplets. This effect may play an important role, as the droplets produced by this mechanism may either collide and aggregate with other settling hail or rain drops, or be entrained into an updraft, to further reinforce the production of hail or large rain drops. The additional latent heat released due to the nucleation of new droplets can feed energy to the existing updraft.

The results presented in this Letter revealed an unexpected mechanism of nucleation and growth of microdroplets in nonequlibirum conditions, such as those in the atmosphere. Our estimates predict that the enhanced nucleation of small droplets by a cold falling drop or ice particle, former clearly observed in the experiments, should also play a role in clouds. It is worth noting that the ideas developed here could be potentially extended to the nucleation of small ice crystals in the wake of large hail particles or graupels. Testing the ideas presented here will require additional experiments and it remains to be seen how this mechanism is affected under turbulent atmospheric conditions.

This work was supported by the German Research Foundation (DFG) Grant No. SFB 937. A. P. acknowledges the support from the Humboldt foundation.

*Corresponding author.
eberhard.bodenschatz@ds.mpg.de
†Corresponding author.
prasanth.prabhakaran@ds.mpg.de

[1] H. Pruppacher and J. Klett, *Microphysics of Clouds and Precipitation* (Springer, New York, 2010).
[2] E. Bodenschatz, S. P. Malinowski, R. A. Shaw, and F. Stratmann, Science **327**, 970 (2010).
[3] R. Narasimha, S. S. Diwan, S. Duvvuri, K. Sreenivas, and G. Bhat, Proc. Natl. Acad. Sci. U.S.A. **108**, 16164 (2011).
[4] E. Bodenschatz, Science **350**, 40 (2015).
[5] A. Pumir and A. Wilkinson, Annu. Rev. Condens. Matter Phys. **7**, 141 (2016).
[6] V. J. Schaefer, Science **104**, 457 (1946).
[7] B. Vonnegut, J. Appl. Phys. **18**, 593 (1947).
[8] I. Langmuir, J. Meteorol. **5**, 175 (1948).
[9] E. B. Kraus and P. Squires, Nature (London) **159**, 489 (1947).
[10] R. T. Bruintjes, Bull. Am. Meteorol. Soc. **80**, 805 (1999).
[11] B. Mason, Contemp. Phys. **23**, 311 (1982).
[12] F. J. Kopp, H. D. Orville, R. D. Farley, and J. H. Hirsch, J. Appl. Meteorol. **22**, 1542 (1983).
[13] P. Ye, A. Bertelsmann, R. H. Heist, B. N. Hale, and M. Kulmala, AIP Conf. Proc. **534**, 19 (2000).
[14] J. R. de Bruyn, E. Bodenschatz, S. W. Morris, S. Trainoff, Y. Hu, D. S. Cannell, and G. Ahlers, Rev. Sci. Instrum. **67**, 2043 (1996).
[15] B. B. Plapp, D. A. Egolf, E. Bodenschatz, and W. Pesch, Phys. Rev. Lett. **81**, 5334 (1998).
[16] S. Weiss, G. Seiden, and E. Bodenschatz, J. Fluid Mech. **756**, 293 (2014).
[17] Phantom 65 Gold Camera, Vision Research.
[18] See Supplemental Material at http://link.aps.org/supplemental/10.1103/PhysRevLett.119.128701, which includes Ref. [19], for additional details and movies.
[19] R. Clift and W. Gauvin, Can. J. Chem. Eng. **49**, 439 (1971).
[20] N. Schaeffer, F. Utheza, F. Garnier, and G. Lauriat, J. Chem. Phys. **113**, 8085 (2000).
[21] F. T. Ferguson, R. H. Heist, and J. A. Nuth, J. Chem. Phys. **132**, 204510 (2010).
[22] J. Feder, K. C. Russell, J. Lothe, and G. M. Pound, Adv. Phys. **15**, 111 (1966).
[23] J. B. Zel'dovich, Acta Physicochim. URSS **18**, 1 (1943).
[24] C. Guder and W. Wagner, J. Phys. Chem. Ref. Data **38**, 33 (2009).
[25] E. W. Lemmon, M. L. Huber, and M. O. McLinden, *NIST Standard Reference Database 23: Reference Fluid Thermodynamic and Transport Properties—REFPROP, Version 9.1* (National Institute of Standards and Technology, Standard Reference Data Program, Gaithersburg, 2013).
[26] Material parameters of SF_6 at $T = 42$ °C: $p_s = 34.715$ bar, $\rho_l = 1053.7$ kg/m^3, $\rho_v = 445.05$ kg/m^3, $M = 146.0554$ g/mol, $\sigma = 0.1629$ mN/m.
[27] S. Whitaker, AIChE J. **18**, 361 (1972).
[28] M. B. de Stadler, N. R. Rapaka, and S. Sarkar, Int. J. Heat Fluid Flow **49**, 2 (2014).
[29] C. F. Bohren and B. A. Albrecht, *Atmospheric Thermodynamics* (Oxford University Press, New York, 1998).
[30] R. Rasmussen, V. Levizzani, and H. Pruppacher, J. Atmos. Sci. **41**, 381 (1984).
[31] B. J. Mason, Q. J. R. Meteorol. Soc. **82**, 209 (1956).
[32] K. Lehmann, H. Siebert, and R. A. Shaw, J. Atmos. Sci. **66**, 3641 (2009).